First Determination of the Level Structure of an *sd*-Shell Hypernucleus, $^{19}_{\Lambda}$F

S. B. Yang,[1,2,*] J. K. Ahn,[3] Y. Akazawa,[4] K. Aoki,[5] N. Chiga,[4] H. Ekawa,[6] P. Evtoukhovitch,[7] A. Feliciello,[8] M. Fujita,[4] S. Hasegawa,[9] S. Hayakawa,[10] T. Hayakawa,[10] R. Honda,[10] K. Hosomi,[9] S. H. Hwang,[11] N. Ichige,[4] Y. Ichikawa,[9] M. Ikeda,[4] K. Imai,[9] S. Ishimoto,[5] S. Kanatsuki,[6] S. H. Kim,[3] S. Kinbara,[12] K. Kobayashi,[10] T. Koike,[4] J. Y. Lee,[1] K. Miwa,[4] T. J. Moon,[1] T. Nagae,[6] Y. Nakada,[10] M. Nakagawa,[10] Y. Ogura,[4] A. Sakaguchi,[10] H. Sako,[9] Y. Sasaki,[4] S. Sato,[9] K. Shirotori,[2] H. Sugimura,[9] S. Suto,[4] S. Suzuki,[5] T. Takahashi,[5] H. Tamura,[4] K. Tanida,[9] Y. Togawa,[4] Z. Tsamalaidze,[7] M. Ukai,[4] T. F. Wang,[13] and T. O. Yamamoto[4]

(J-PARC E13 Collaboration)

[1]*Department of Physics and Astronomy, Seoul National University, Seoul 08826, Korea*
[2]*Research Center for Nuclear Physics (RCNP), Osaka University, Ibaraki, Osaka 567-0047, Japan*
[3]*Department of Physics, Korea University, Seoul 02841, Korea*
[4]*Department of Physics, Tohoku University, Sendai 980-8578, Japan*
[5]*Institute of Particle and Nuclear Studies (IPNS), High Energy Accelerator Research Organization (KEK), Tsukuba 305-0801, Japan*
[6]*Department of Physics, Kyoto University, Kyoto 606-8502, Japan*
[7]*Joint Institute for Nuclear Research, Dubna, Moscow Region 141980, Russia*
[8]*INFN, Sezione di Torino, via P. Giuria 1, 10125 Torino, Italy*
[9]*Advanced Science Research Center (ASRC), Japan Atomic Energy Agency (JAEA), Tokai, Ibaraki 319-1195, Japan*
[10]*Department of Physics, Osaka University, Toyonaka, Osaka 560-0043, Japan*
[11]*Korea Research Institute of Standards and Science (KRISS), Daejeon 34113, Korea*
[12]*Faculty of Education, Gifu University, Gifu 501-1193, Japan*
[13]*Research Center of Nuclear Science and Technology (RCNST) and School of Physics and Nuclear Energy Engineering, Beihang University, Beijing 100191, China*

(Received 20 December 2017; revised manuscript received 15 February 2018; published 29 March 2018)

We report on the first observation of γ rays emitted from an *sd*-shell hypernucleus, $^{19}_{\Lambda}$F. The energy spacing between the ground state doublet, $1/2^+$ and $3/2^+$ states, of $^{19}_{\Lambda}$F is determined to be $315.5 \pm 0.4(\mathrm{stat})^{+0.6}_{-0.5}(\mathrm{syst})$ keV by measuring the γ-ray energy of the $M1(3/2^+ \to 1/2^+)$ transition. In addition, three γ-ray peaks are observed and assigned as $E2(5/2^+ \to 1/2^+)$, $E1(1/2^- \to 1/2^+)$, and $E1(1/2^- \to 3/2^+)$ transitions. The excitation energies of the $5/2^+$ and $1/2^-$ states are determined to be $895.2 \pm 0.3(\mathrm{stat}) \pm 0.5(\mathrm{syst})$ and $1265.6 \pm 1.2(\mathrm{stat})^{+0.7}_{-0.5}(\mathrm{syst})$ keV, respectively. It is found that the ground state doublet spacing is well described by theoretical models based on existing *s*- and *p*-shell hypernuclear data.

DOI: 10.1103/PhysRevLett.120.132505

The spectroscopy of Λ hypernuclei has played an essential role in the recent trend of nuclear physics extending nuclear forces and nuclear systems to baryon-baryon interactions and baryonic many body systems [1–3]. Since the ΛN scattering data are quite limited due to the short lifetime of the Λ hyperon, experimental data on the structure of Λ hypernuclei have also been used to extract information on the ΛN interaction. In particular, precise energy level values obtained via γ-ray spectroscopy for *s*- and *p*-shell hypernuclei have revealed the strengths of the spin-dependent ΛN interactions, by comparing them with those calculated from assumed baryon-baryon interactions [4–9]. It is also found that the phenomenological spin-dependent interaction parameters determined from a few *p*-shell hypernuclear levels successfully reproduce almost all the *p*-shell hypernuclear level data [10].

It is interesting to ask whether the ΛN spin-dependent interactions that successfully describe *s*- and *p*-shell hypernuclei can also be applied to heavier hypernuclei, since the wave function overlap between a Λ in the $0s$ orbit and valence nucleons in the outermost orbit is expected to be different among *s*-, *p*-, and heavier hypernuclei. In addition, the three-body ΛNN interaction that originates from the ΛN-ΣN coupling plays a particularly important role in the structure of *s*- and *p*-shell hypernuclei [11–13], and it is also interesting to investigate how the coupling effect changes in heavier hypernuclei [12]. Thus, experimental results on various hypernuclei beyond *s*- and *p*-shell hypernuclei have been anticipated. The extension of the spectroscopic study from *s*- and *p*-shell hypernuclei to *sd*-shell and heavier hypernuclei will allow us to test our theoretical

frameworks for hypernuclear structure and our knowledge of the ΛN interaction.

This Letter reports the first experimental investigation of *sd*-shell hypernuclear structure via precise γ-ray spectroscopy using germanium (Ge) detectors. We selected ${}^{19}_{\Lambda}$F as the first target of *sd*-shell hypernuclei, because ${}^{19}_{\Lambda}$F has a structure of ${}^{16}\mathrm{O} + p + n + \Lambda$, being similar to the well known ${}^{7}_{\Lambda}$Li (${}^{4}\mathrm{He} + p + n + \Lambda$) [4,7,14]. The ground state ($J^{\pi} = 1^{+}$) of ^{18}F is split in the ${}^{19}_{\Lambda}$F hypernucleus by the spin of the additional Λ as shown in Fig. 1. The energy spacing between the members of the ground state doublet, $1/2^{+}$ and $3/2^{+}$, is largely determined by the spin-spin ΛN interaction because of the dominant $S = 1$ and $L = 0$ structure of ^{18}F (1^{+}), as in the ground state doublet of ${}^{7}_{\Lambda}$Li ($3/2^{+}, 1/2^{+}$). By measuring the γ-ray energy of the spin-flip $M1$ transition [${}^{19}_{\Lambda}\mathrm{F}(3/2^{+} \rightarrow 1/2^{+})$], the strength of the effective spin-spin interaction in the *sd*-shell hypernucleus can be obtained, and it can be directly compared with the effective spin-spin interaction for the *s*- and *p*-shell hypernuclei. The structure of ${}^{19}_{\Lambda}$F has been theoretically studied via the shell model [10,15]; in Ref. [15] the cross sections of ${}^{19}_{\Lambda}$F excited states populated via the (K^{-}, π^{-}) reaction and their γ-transition strengths are also calculated.

The experiment (J-PARC E13 Collaboration, γ-ray spectroscopy of ${}^{4}_{\Lambda}$He and ${}^{19}_{\Lambda}$F [16]) was performed at the K1.8 beam line in the J-PARC Hadron Experimental Facility [17]. We have already reported the result of ${}^{4}_{\Lambda}$He γ-ray spectroscopy [9]. The experimental setup of the ${}^{19}_{\Lambda}$F study was the same as in the ${}^{4}_{\Lambda}$He case, except for the beam momentum and the target.

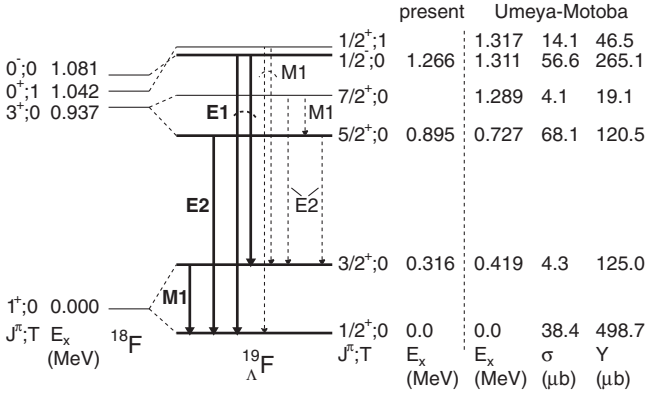

FIG. 1. Low-lying level scheme and γ transitions of ${}^{19}_{\Lambda}$F. "Present" indicates the measured excitation energy and the thick arrows indicate observed transitions in this experiment. Dashed arrows show possible other transitions expected in this level scheme. Results of the theoretical calculation by Umeya and Motoba [15] are also shown. σ is the production cross section by the (K^{-}, π^{-}) reaction at 1.8 GeV/c, integrated between 0° and 12° in the laboratory frame. Y is the sum of the yield of the direct production and the population via γ cascades from higher states below $E_x = 6$ MeV.

The ${}^{19}_{\Lambda}$F hypernuclei were produced by the ${}^{19}\mathrm{F}(K^{-}, \pi^{-})$ reaction with a 1.8 GeV/c kaon beam and a 20 g/cm^2-thick liquid CF_4 target. The beam line spectrometer and the Superconducting Kaon Spectrometer (SKS) [18] were used to identify ${}^{19}_{\Lambda}$F production, and at the same time γ rays were detected with a Ge detector array, Hyperball-J [19]. The intensity of the kaon beam was typically 3.5×10^5 per one spill (2 s) occurring every 6 s and a typical K^{-}/π^{-} ratio was 2.5. The target was irradiated with a total of 6.3×10^{10} kaons.

The momenta and trajectories of beam kaons were measured by the beam line spectrometer. The beam kaons were identified at the trigger level by two aerogel Čerenkov counters installed in front of the target. The misidentification probability of the beam kaons was less than 1%. A muon filter and a π^0 veto counter were used to reject the decays of the beam kaons, $K^{-} \rightarrow \mu^{-}\bar{\nu}_{\mu}$ and $K^{-} \rightarrow \pi^{-}\pi^{0}$, respectively. These veto counters made the trigger rate sufficiently low. For the outgoing pions, the SKS was used for measuring the momenta and trajectories. The outgoing pions were identified by an aerogel Čerenkov counter, installed just downstream of the target, at the trigger level and by the time-of-flight technique in the off-line analysis. Through the off-line analysis, pions were well separated from other particles except for muons from the K^{-} beam decay. More detailed descriptions of the experimental setup can be found in Refs. [9,20].

The reconstructed momenta of the beam and outgoing particles were calibrated to reproduce the mass of Σ^{+} [21] and the Λ binding energy of the ${}^{12}_{\Lambda}$C ground state [22] produced by the (K^{-}, π^{-}) reaction with a CH_2 target. After the momentum calibration, the missing mass accuracy was estimated to be ± 1 MeV/c^2.

Hyperball-J consisted of 27 coaxial-type Ge detectors having a crystal size of 70 mm(ϕ) × 70 mm. The absolute photopeak efficiency taking the absorption in the target material into account was 3% for 1 MeV γ rays. At least one hit in the Ge detectors was requested for the trigger conditions. In the off-line analysis, Ge detector events in coincidence with the (K^{-}, π^{-}) reaction were selected by using a timing gate that depends on the γ-ray energy. Each of the Ge detectors was surrounded by $PbWO_4$ counters to suppress backgrounds from Compton scattering inside of the Ge crystal and from π^0 decay. We rejected those events in which the Ge detectors have hits in coincidence with the surrounding $PbWO_4$ counters.

The energy calibration of the Ge detectors was performed by using a natural radioactive ^{232}Th source in the off-beam periods between beam spills and known γ rays from nuclei inside the target or the surrounding materials during beam spills. After the energy calibration, we achieved an accuracy of 0.5 keV for the γ-ray energy range from 0.1 to 2.6 MeV, which gives the dominant systematic uncertainty for the γ-ray energies. The energy resolution of the Ge detectors was measured to be 4.5 keV

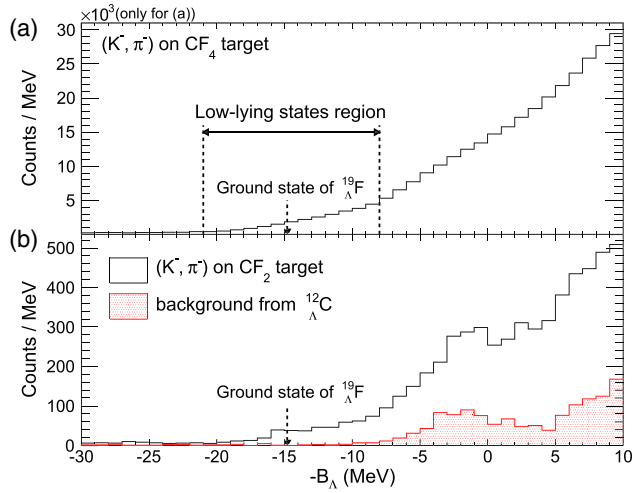

FIG. 2. Hypernuclear mass spectra of ${}^{19}_{\Lambda}$F with (a) the liquid CF_4 target (20 g/cm^2) and (b) the CF_2 (Teflon) target (6.6 g/cm^2), plotted in the Λ binding energy (B_Λ). Only in (a), events are requested to have at least one hit in the Ge detectors. The ground state energy of ${}^{19}_{\Lambda}$F and the low-lying states region described in the text are marked. In (b), the shaded area indicates the background from ${}^{12}_{\Lambda}$C.

(FWHM) for 1 MeV γ rays. The variation of the γ-ray peak shape due to the Doppler broadening effect for the ${}^{19}_{\Lambda}$F in flight was estimated by using a MC simulation based on GEANT4 [23] and the SRIM code [24] for deceleration of ${}^{19}_{\Lambda}$F in the CF_4 target. We used the results of the MC simulation to distinguish between in-flight and at-rest γ-ray emission and to assign the γ transition.

We selected the reaction angle (θ) range of $2° < \theta < 12°$, due to the large background from the beam decays at angles smaller than 2° and the small production cross section for ${}^{19}_{\Lambda}$F at angles larger than 12°. In addition, we also acquired data samples with a 6.6 g/cm^2 CF_2 (Teflon) target to verify the ${}^{19}_{\Lambda}$F production with a better missing mass resolution and without the γ-ray hit bias in the trigger conditions.

Figure 2 shows the mass spectra for (a) the thick CF_4 target, and (b) the thin CF_2 target plotted in the Λ binding energy (B_Λ) scale. The ground state of ${}^{19}_{\Lambda}$F is expected to be at $-B_\Lambda = -14.8$ MeV [15]. In Figs. 2(a) and 2(b), the spectra have significant numbers of events around the ${}^{19}_{\Lambda}$F ground state energy and above, indicating the production of low-lying s_Λ states of ${}^{19}_{\Lambda}$F, although the peaks are not clearly seen due to the insufficient missing mass resolution [8.7 MeV FWHM in (a) and 5.9 MeV FWHM in (b)]. As shown in Fig. 2(a), we selected the B_Λ range of $-21 < -B_\Lambda < -8$ MeV (the "low-lying states region") in order to observe γ rays emitted from the ${}^{19}_{\Lambda}$F low-lying states as given in Fig. 1. This region does not cover all the excited states that can populate the low-lying states through γ cascades. However, we did not extend the region to avoid background γ rays from hyperfragments such as ${}^{15}_{\Lambda}$N, ${}^{18}_{\Lambda}$O, or ${}^{18}_{\Lambda}$F after α, p, or n emissions from p_Λ or highly excited states of ${}^{19}_{\Lambda}$F; the expected energy for the p_Λ states and the lowest particle emission threshold for hyperfragments are $-B_\Lambda \cong -4$ and -9 MeV, respectively [15], and thus all the p_Λ states of ${}^{19}_{\Lambda}$F decay into hyperfragments. In addition, ${}^{12}_{\Lambda}$C states produced on ^{12}C in the CF_4 target also contribute to the background at $-B_\Lambda \gtrsim -8$ MeV in the ${}^{19}_{\Lambda}$F mass spectrum, as confirmed by the red histogram in Fig. 2(b), which was obtained from CH_2 target data taken with the same setup and analyzed with the ${}^{19}\mathrm{F}(K^-, \pi^-)$ kinematics.

Figure 3 shows the γ-ray spectra for various B_Λ regions: (a) the "highly unbound region" ($20 < -B_\Lambda < 200$ MeV), (b) the "highly excited states region" ($-8 < -B_\Lambda < 5$ MeV), and (c) the low-lying states region. Several known γ rays from ordinary nuclei such as ^{19}F, ^{18}F, etc. are seen in all the spectra as expected for background γ rays. The highly excited states region was selected to identify γ-ray peaks that were emitted from high excited states including p_Λ states and hyperfragments. In (b), we observed two unknown γ-ray peaks with 270 and 1029 keV energies, and their sources are considered as hyperfragments. After gating the low-lying states region, three peaks appeared at 316, 895, and 1266 keV in the γ-ray spectrum (c), with statistical significances of more than 3σ.

The γ-ray peak at 316 keV is attributed to the $M1(3/2^+ \to 1/2^+)$ transition between the ground state doublet members, because the yield of the $3/2^+ \to 1/2^+$ $M1$ transition is expected to be more than 10 times larger than the other transitions in the 100–500 keV energy range [15]. The energy and width of the γ-ray peak are determined to be $315.5 \pm 0.4(\mathrm{stat})^{+0.6}_{-0.5}(\mathrm{syst})$ keV and $5.0 \pm 0.9^{+0.5}_{-0.3}$ keV (FWHM), respectively.

As shown in Fig. 3(c), the peak at 895 keV exhibits a narrow width, $4.3 \pm 0.5(\mathrm{stat})^{+0.1}_{-0.2}(\mathrm{syst})$ keV (FWHM), which is consistent with the energy resolution of the Ge detectors, $4.5^{+0.4}_{-0.3}$ keV (FWHM). It indicates that the γ rays are emitted after the ${}^{19}_{\Lambda}$F hypernucleus has completely stopped. By comparing it with expected lifetimes and cross sections of ${}^{19}_{\Lambda}$F states [15], this γ-ray peak is attributed to the $E2(5/2^+ \to 1/2^+)$ or $E1(1/2^- \to 3/2^+)$ transitions. Here, the latter assignment is rejected because $E1(1/2^- \to 1/2^+)$ is not seen at 1.21 MeV in spite of the expected branching ratio, $\mathrm{BR}(1/2^- \to 1/2^+)/\mathrm{BR}(1/2^- \to 3/2^+) = 1.7$. A peak from the $5/2^+ \to 3/2^+$ γ transition is not clearly seen at 580 keV in Fig. 3(c), but it is consistent with the fact that the $M1(5/2^+ \to 3/2^+)$ transition is largely suppressed in the weak coupling limit. From a fit to the 895 keV peak, the energy of the $E2(5/2^+ \to 1/2^+)$ transition is derived as $895.2 \pm 0.3(\mathrm{stat}) \pm 0.5(\mathrm{syst})$ keV.

We considered the γ transition of the 1266 keV peak in Fig. 3(c) as the $E1(1/2^- \to 1/2^+)$ transition due to the expected large cross section of the $1/2^-$ state [15]. To confirm this assignment, the events with forward reaction angles of 2°–6° were selected, since the cross section of the

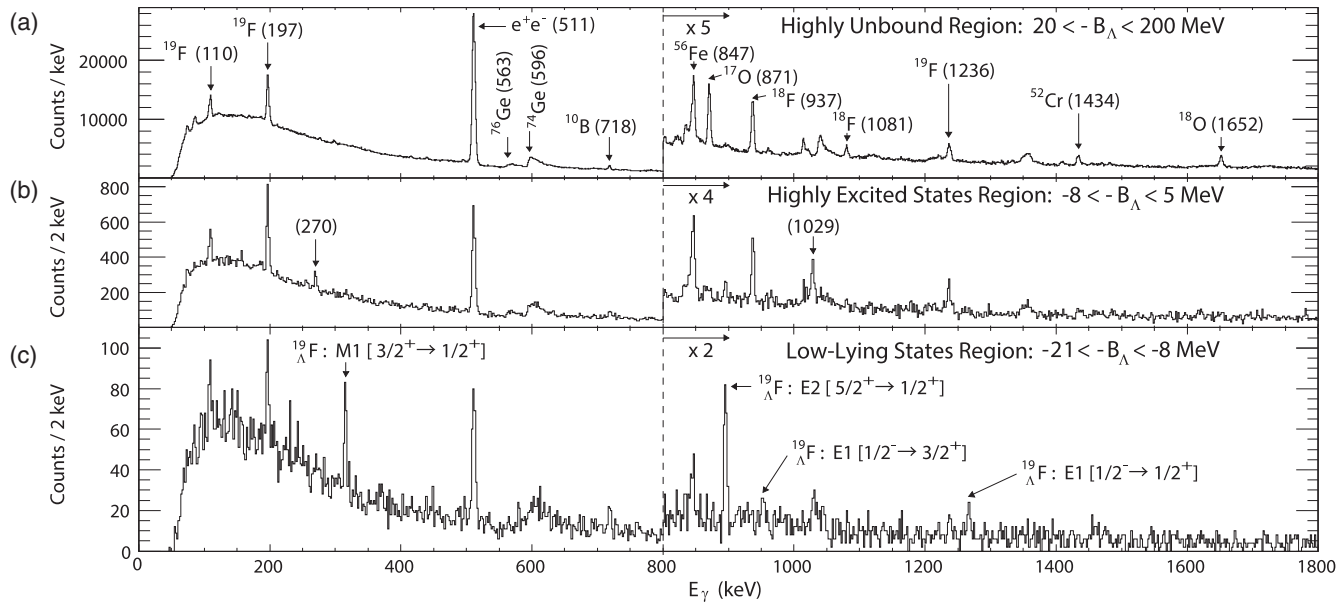

FIG. 3. γ-ray energy spectra gated by Λ binding energy ranges: (a) unbound region ($20 < -B_\Lambda < 200$ MeV), (b) highly excited states region ($-8 < -B_\Lambda < 5$ MeV), and (c) low-lying states region ($-21 < -B_\Lambda < -8$ MeV). Several γ-ray peaks from ordinary nuclei are marked with their source in (a). Two new γ-ray peaks at 270 and 1029 keV are shown in (b). In (c), two γ rays at 316 and 895 keV are assigned as $M1(3/2^+ \to 1/2^+)$ and $E2(5/2^+ \to 1/2^+)$ transitions, respectively (see text). Other two γ-ray peaks at 953 and 1266 keV, assigned as $E1$ transitions, are magnified in Fig. 4.

$1/2^-$ state is expected to be the largest at 4° [15]. At the forward reaction angles, as shown in Fig. 4(b), the peak is more evident and another peak at 953 keV is also seen with a statistical significance of 3.2σ. From a fit to the γ-ray spectrum, the energies of the two peaks are determined to be $952.8 \pm 1.2(\text{stat})^{+0.5}_{-0.6}(\text{syst})$ and $1265.6 \pm 1.2(\text{stat})^{+0.7}_{-0.5}(\text{syst})$ keV. The energy difference between the two peaks, $312.7 \pm 1.7(\text{stat})$ keV, is consistent with the energy spacing between the ground state doublet, which is found to be $315.5 \pm 0.4(\text{stat})$ keV as described above. It indicates that the 953 and 1266 keV γ rays are emitted from the same initial state decaying to the $3/2^+$ and $1/2^+$ states, respectively. Therefore, we assigned the peaks to the $E1(1/2^- \to 3/2^+)$ and $E1(1/2^- \to 1/2^+)$ transitions. The measured yields and the widths of the γ rays support this assignment. By using the calculated transition probabilities of $B(E1; 1/2^- \to 3/2^+, 1/2^+)$ [15], the yield of the 953 keV γ ray was estimated to be 18 ± 6 events from the measured yield of the 1266 keV γ ray, $25 \pm 8(\text{stat})^{+2}_{-5}(\text{syst})$ events, and a relative Hyperball-J efficiency for the different γ-ray energies. The estimated yield is consistent with the measured yield, $19 \pm 8(\text{stat})^{+1}_{-2}(\text{syst})$ events. Additionally, the widths of the 953 and 1266 keV peaks, $5.9 \pm 2.1(\text{stat})^{+0.2}_{-0.1}(\text{syst})$ and $8.1 \pm 3.0(\text{stat})^{+0.5}_{-0.6}(\text{syst})$ keV (FWHM), respectively, are consistent with the detector resolution [$4.5^{+0.4}_{-0.3}$ and $4.7^{+0.4}_{-0.3}$ keV (FWHM), respectively]. Because of the very slow core transition of $^{18}\text{F}(0^- \to 1^+)$, these $E1$ transitions of $^{19}_\Lambda$F are almost unbroadened by a Doppler shift, while the $M1[1/2^+(T=1) \to 3/2^+, 1/2^+]$ transitions in Fig. 1 are Doppler broadened and expected to have widths of $10.8^{+0.5}_{-0.3}$ and $14.0^{+0.7}_{-0.4}$ keV (FWHM), respectively, according to the MC simulation.

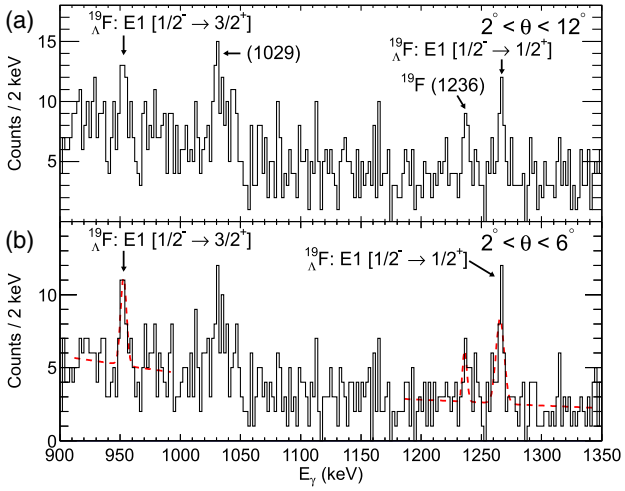

FIG. 4. γ-ray spectra for the low-lying states region, $-21 < -B_\Lambda < -8$ MeV. (a) shows the enlargement of Fig. 3(c) from 900 to 1350 keV. In (b), the forward reaction angles of $2° < \theta < 6°$ are selected. Two γ-ray peaks are observed at 953 and 1266 keV, which are assigned as $E1(1/2^- \to 3/2^+)$ and $E1(1/2^- \to 1/2^+)$, respectively. The dotted lines in (b) show fitting results.

The measured $(3/2^+, 1/2^+)$ doublet spacing of 316 keV is in good agreement with the two independent shell-model

calculations so far. It is noted that both calculations reproduce the spacing energies of spin-spin doublets for s- and p-shell hypernuclei. Millener predicted the spacing energy to be 305 keV from the phenomenological spin-dependent ΛN interaction strengths determined from the p-shell hypernuclear data [10]. Since the $\Lambda\Sigma$ coupling effect is not included in this calculation, the agreement suggests that the coupling effect to the hypernuclear spin-spin doublet spacing, which is significantly large in the s-shell hypernuclei [11] and smaller in the p-shell hypernuclei [10,13], is negligibly small in the sd-shell hypernuclei. It is consistent with what is suggested in Ref. [12].

On the other hand, the shell-model calculation by Umeya and Motoba with the effective ΛN interaction obtained from the Nijmegen SC97e and SC97f interactions via the G-matrix method predicts the spacing of 245 keV [25] and 419 keV [15], respectively. The situation is quite similar to the case of the $A = 4$ and 7 hypernuclei. For the ground-state doublet spacing of ${}^{7}_{\Lambda}$Li ($3/2^+$, $1/2^+$; 0.692 MeV) [4], the Nijmegen G-matrix interaction gives 0.348 MeV (SC97e) and 0.942 MeV (SC97f) [25], and for the spacings of ${}^{4}_{\Lambda}$H and ${}^{4}_{\Lambda}$He (1^+, 0^+; 1.25 MeV in average for ${}^{4}_{\Lambda}$H and ${}^{4}_{\Lambda}$He) [9], it gives 0.89 MeV (SC97e) and 1.48 MeV (SC97f) [11]. In addition, these agreements indicate that the weak coupling assumption between a $0s$-state Λ and the core nucleus, one of the most basic concepts in Λ-hypernuclear structure, is still valid in sd-shell hypernuclei.

In summary, we observed γ rays from an sd-shell Λ hypernucleus, ${}^{19}_{\Lambda}$F, for the first time. The energy spacing between the $3/2^+$ and $1/2^+$ states is determined to be $315.5 \pm 0.4(\mathrm{stat})^{+0.6}_{-0.5}(\mathrm{syst})$ keV, as well as the excitation energies of the $5/2^+$ and $1/2^-$ states. The $(3/2^+, 1/2^+)$ energy spacing is well reproduced by the ΛN spin-dependent interactions which reproduced the s- and p-shell hypernuclear data. It also suggests that the $\Lambda\Sigma$ coupling effect is diminished in heavier hypernuclei. Our result shows that the present theoretical frameworks work quite successfully in describing the structure of not only light s- and p-shell hypernuclei but also a heavier one beyond p-shell hypernuclei. Such precise spectroscopic studies of light to heavy Λ hypernuclei would also provide a unique means to investigate the nuclear density dependence of the baryon-baryon interactions in nuclear matter.

We thank the J-PARC accelerator and facility staff and all the project members who participated in the development of the SKS and Hyperball-J. We also thank A. Umeya, T. Motoba, and D. J. Millener for their theoretical calculations of ${}^{19}_{\Lambda}$F. This work is partially supported by Tohoku University's Focused Research Project, and Grants-in-Aid No. 17070001, No. 21684011, No. 23244043, No. 24105003, No. 24740138, and No. 15H02079 for Scientific Research from the Ministry of Education, Culture, Sports, Science and Technology (MEXT) Japan. This research is also supported by World Class University program (Grant No. R32-10155), Basic Research (Young Researcher) (Grant No. 2010-0004752), Center for Korean J-PARC Users (Grants No. K2100200173811B130002410 and No. NRF-2013K1A3A7A06056592), and Brain Korea 21 Plus program through National Research Foundation (NRF) of Korea.

*Present Address: Research Center for Nuclear Physics (RCNP), Osaka University, Ibaraki, Osaka 567-0047, Japan.

[1] A. Gal, E. V. Hungerford, and D. J. Millener, Rev. Mod. Phys. **88**, 035004 (2016).
[2] Y. Yamamoto, Th. A. Rijken, and T. Motoba, Prog. Theor. Phys. Suppl. **185**, 72 (2010); E. Hiyama, M. Kamimura, Y. Yamamoto, T. Motoba, and Th. A. Rijken, *ibid.* **185**, 106 (2010).
[3] O. Hashimoto and H. Tamura, Prog. Part. Nucl. Phys. **57**, 564 (2006).
[4] H. Tamura *et al.*, Phys. Rev. Lett. **84**, 5963 (2000).
[5] H. Akikawa *et al.*, Phys. Rev. Lett. **88**, 082501 (2002).
[6] M. Ukai *et al.*, Phys. Rev. Lett. **93**, 232501 (2004).
[7] M. Ukai *et al.*, Phys. Rev. C **73**, 012501(R) (2006).
[8] M. Ukai *et al.*, Phys. Rev. C **77**, 054315 (2008).
[9] T. O. Yamamoto *et al.*, Phys. Rev. Lett. **115**, 222501 (2015).
[10] D. J. Millener, Nucl. Phys. **A914**, 109 (2013).
[11] See Y. Akaishi, T. Harada, S. Shinmura, and K. S. Myint, Phys. Rev. Lett. **84**, 3539 (2000) and references therein.
[12] A. Gal and D. J. Millener, Phys. Lett. B **725**, 445 (2013).
[13] R. Wirth and R. Roth, Phys. Rev. Lett. **117**, 182501 (2016).
[14] K. Tanida *et al.*, Phys. Rev. Lett. **86**, 1982 (2001).
[15] A. Umeya and T. Motoba, Nucl. Phys. **A954**, 242 (2016).
[16] H. Tamura, M. Ukai, T.O. Yamamoto, and T. Koike, Nucl. Phys. **A881**, 310 (2012).
[17] K. Agari *et al.*, Prog. Theor. Exp. Phys. **2012**, 02B009 (2012).
[18] T. Takahashi *et al.*, Prog. Theor. Exp. Phys. **2012**, 02B010 (2012).
[19] T. Koike *et al.*, in *Proceedings of the 9th International Conference on Hypernuclear and Strange Particle Physics (HYP2006), Mainz, Germany, 2006*, edited by J. Pochodzalla and T. Walcher (Springer, New York, 2007), p. 25.
[20] S. B. Yang *et al.*, JPS Conf. Proc. **1**, 013076 (2014).
[21] K. A. Olive *et al.* (Particle Data Group), Chin. Phys. C **38**, 090001 (2014).
[22] T. Gogami *et al.*, Phys. Rev. C **93**, 034314 (2016).
[23] J. Allison, K. Amako, J. Apostolakis, H. Araujo, P. Dubois *et al.* (GEANT4 Collaboration), IEEE Trans. Nucl. Sci. **53**, 270 (2006); S. Agostinelli *et al.* (GEANT4 Collaboration), Nucl. Instrum. Methods Phys. Res., Sect. A **506**, 250 (2003).
[24] J. Ziegler, SRIM (Stopping Range of Ions in Matter) 2013.00, http://srim.org.
[25] A. Umeya and T. Motoba (private communication), calculations similar to Ref. [15].